



HAL
open science

Nuclear Quantum Effects in Water Reorientation and Hydrogen-Bond Dynamics

David Mark Wilkins, David E. Manolopoulos, Silvio Pipolo, Damien Laage,
James T. Hynes

► **To cite this version:**

David Mark Wilkins, David E. Manolopoulos, Silvio Pipolo, Damien Laage, James T. Hynes. Nuclear Quantum Effects in Water Reorientation and Hydrogen-Bond Dynamics. *Journal of Physical Chemistry Letters*, 2017, 10.1021/acs.jpcllett.7b00979 . hal-01527210

HAL Id: hal-01527210

<https://hal.sorbonne-universite.fr/hal-01527210v1>

Submitted on 24 May 2017

HAL is a multi-disciplinary open access archive for the deposit and dissemination of scientific research documents, whether they are published or not. The documents may come from teaching and research institutions in France or abroad, or from public or private research centers.

L'archive ouverte pluridisciplinaire **HAL**, est destinée au dépôt et à la diffusion de documents scientifiques de niveau recherche, publiés ou non, émanant des établissements d'enseignement et de recherche français ou étrangers, des laboratoires publics ou privés.

Nuclear Quantum Effects in Water Reorientation and Hydrogen-Bond Dynamics

David M. Wilkins,^{*,†} David E. Manolopoulos,^{*,‡} Silvio Pipolo,^{*,¶,§,||} Damien
Laage,^{*,¶,||} and James T. Hynes^{*,¶,⊥}

[†]*Laboratory of Computational Science and Modeling, IMX, École Polytechnique Fédérale de
Lausanne, 1015 Lausanne, Switzerland*

[‡]*Physical and Theoretical Chemistry Laboratory, University of Oxford, South Parks Road,
Oxford OX1 3QZ, UK*

[¶]*PASTEUR, Département de Chimie, École Normale Supérieure, UPMC Univ Paris 06,
CNRS, PSL Research University, 75005 Paris, France*

[§]*Current address: Unité de Catalyse et Chimie du Solide, Université de Lille 1, 59655
Villeneuve d'Ascq, France*

^{||}*Sorbonne Universités, UPMC Univ Paris 06, ENS, CNRS, PASTEUR, 75005 Paris, France*

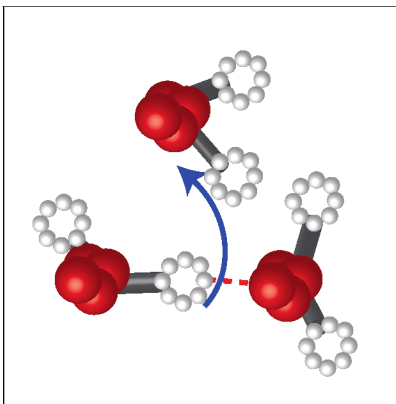
[⊥]*Department of Chemistry and Biochemistry, University of Colorado, Boulder, CO
80309-0215, USA*

E-mail: david.wilkins@epfl.ch; david.manolopoulos@chem.ox.ac.uk; silvio.pipolo@univ-lille1.fr;
damien.laage@ens.fr; james.hynes@colorado.edu

Abstract

We combine classical and ring polymer molecular dynamics simulations with the molecular jump model to provide a molecular description of the nuclear quantum effects (NQEs) on water reorientation and hydrogen-bond dynamics in liquid H₂O and D₂O. We show that while the net NQE is negligible in D₂O, it leads to a ~13% acceleration in H₂O dynamics compared to a classical description. Large angular jumps exchanging hydrogen-bond partners are the dominant reorientation pathway (just as in a classical description); the faster reorientation dynamics arise from the increased jump rate constant. NQEs do not change the jump amplitude distribution and no significant tunneling is found. The faster jump dynamics are quantitatively related to decreased structuring of the OO radial distribution function when NQEs are included. This is explained, via a jump model analysis, by a competition between the effects of water's librational and OH stretch mode zero point energies on the hydrogen-bond strength.

Graphical TOC Entry



1
2
3
4
5
6
7
8
9
10
11
12
13
14
15
16
17
18
19
20
21
22
23
24
25
26
27
28
29
30
31
32
33
Water reorientation and hydrogen-bond (H-bond) network rearrangements are essential for a broad range of chemical and biochemical processes in aqueous solution, including proton transfer reactions, ion transport, protein folding and ligand-biomolecule binding.¹⁻⁴ Since these water motions involve displacements of hydrogens with very small mass, an explicit description of quantum mechanical zero point energy and tunneling effects may be necessary.^{5,6} Indeed, recent simulations have established that competing nuclear quantum effects (NQEs) on the intra- and intermolecular interactions^{7,8} lead to a net acceleration of water translational and rotational dynamics.^{7,9-11} In the case of the rotational dynamics, it has been argued^{12,13} on the basis of classical simulations that water reorientation proceeds via a mechanism involving sudden large angular jumps, in which H-bonding partners are exchanged during, in effect, a chemical reaction, a mechanism that is in strong contrast to the traditional Debye diffusion picture. If this jump mechanism also applies to quantum water, it could provide a detailed molecular picture of the factors responsible for the quantum rotational acceleration. But in fact, the relevance of the jump mechanism for water has been questioned, precisely because of the possible role of NQEs (see, e.g., refs 11,14).

34
35
36
37
38
39
40
41
42
43
44
45
46
47
Here we address these issues via classical molecular dynamics (MD) and – for the quantum case – thermostatted ring polymer molecular dynamics (TRPMD)¹⁵ simulations of H₂O and D₂O water reorientation and associated H-bond dynamics. We show that the molecular jump mechanism^{12,13} remains valid when NQEs are included, and that the dynamical acceleration induced by NQEs arises from faster H-bond jump exchanges within this mechanism. Finally, we establish that the isotope and NQEs on jump dynamics can be quantitatively inferred from the changes in the oxygen-oxygen radial distribution function.

48
49
50
51
52
53
54
55
56
57
58
59
60
All our simulations employ the flexible q-TIP4P/F potential.⁷ While more sophisticated potentials are now available (e.g., MB-pol¹⁶), they are more expensive to evaluate; moreover since q-TIP4P/F has been shown to reproduce the experimental structural and dynamical properties of liquid water when NQEs are included,⁷ it is ideal for present purposes. For both H₂O and D₂O, 216 water molecules are simulated at the experimental density¹⁷ at 298 K and

propagated in 50 independent 3 ns classical NVE runs and 20 independent 500 ps quantum TRPMD¹⁵ trajectories.

The water reorientation dynamics are probed by the orientation time-correlation functions,

$$C_n(t) = \langle P_n[\mathbf{u}_{\text{OH}}(0) \cdot \mathbf{u}_{\text{OH}}(t)] \rangle, \quad (1)$$

where $\mathbf{u}_{\text{OH}}(t)$ is the water OH (or OD) bond's orientation at time t and P_n is the n^{th} order Legendre polynomial (see SI for their calculation within the RPMD approach). These are shown for $n=1-3$ in fig 1. Although only C_2 is experimentally accessible,¹⁸ we also consider C_1 and C_3 since different orders have been suggested⁷ to exhibit different NQEs. Following ref 13, we focus on the reorientation beyond the initial sub-ps librational decay and determine the reorientation times τ_n by an exponential fit of $C_n(t)$ to Ae^{-t/τ_n} for $4 \leq t \leq 15$ ps.

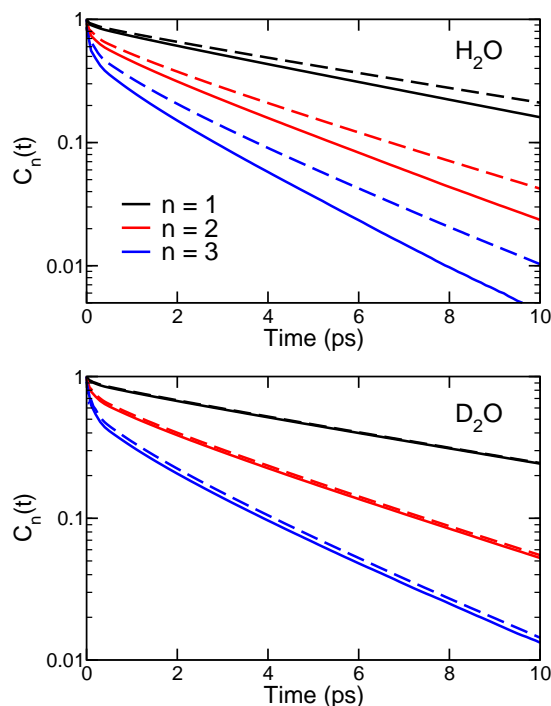


Figure 1: Orientation correlation functions $C_n(t)$ [eq 1] for $n = 1, 2, 3$ for H_2O (upper panel) and D_2O (lower panel), from classical (dashes) and TRPMD (solid lines) simulations.

In H_2O , Table 1's τ_n times show that, in agreement with previous studies,^{7,9-11} NQEs

Table 1: Reorientation times τ_n , jump time τ_0 , inverse of frame rotational diffusion coefficient $1/D_R^{\text{frame}}$ and EJM reorientation times τ_n^{EJM} (eq 2), from classical MD (cl) and TRPMD (qm) simulations, together with their ratios (all times in ps).

	H ₂ O			D ₂ O		
	cl	qm	qm/cl	cl	qm	qm/cl
τ_1	7.1(2)	6.1(1)	0.85(3)	8.0(3)	8.0(3)	1.00(5)
τ_2	3.7(1)	3.16(7)	0.86(4)	4.1(1)	4.12(7)	1.00(4)
τ_3	2.7(1)	2.26(4)	0.85(4)	2.9(1)	2.98(7)	1.02(5)
τ_0	4.4(1)	3.83(4)	0.87(3)	4.9(1)	4.87(5)	1.00(3)
$1/D_R^{\text{frame}}$	52(1)	45(1)	0.86(3)	56(2)	59(2)	1.04(5)
τ_1^{EJM}	7.1(1)	6.16(6)	0.87(2)	8.0(2)	8.0(1)	1.01(3)
τ_2^{EJM}	3.15(7)	2.73(3)	0.87(2)	3.50(7)	3.54(5)	1.01(3)
τ_3^{EJM}	2.09(4)	1.81(2)	0.87(2)	2.30(5)	2.34(4)	1.01(3)

accelerate water reorientational dynamics. An interesting feature is that the acceleration factor $\rho_n = \tau_n^{\text{qm}}/\tau_n^{\text{cl}}$ is independent of the order n of the orientational time-correlation function (tcf), and very similar to the value of 0.87 previously found⁷ for the NQE on the translational dynamics of the same q-TIP4P/F model, suggesting a common origin for the NQE acceleration of rotational and translational dynamics. Our results further show that the increase of ρ_n with n found in ref. 7 is actually caused by the sub-ps librational (hindered rotational) water molecular motions and not by the longer-time reorientation dynamics. As detailed in the SI, in contrast with our longer time τ_n values, the integrated reorientation times $\int_0^\infty C_n(t) dt$ considered in ref. 7 include the initial librational decay. Librations make a growing contribution to the integrated times for increasing n ; their amplitude's strong sensitivity to NQEs results in the observed increase with n of those times' quantum/classical acceleration (see SI).

Turning to D₂O, Table 1 shows that reorientation times are not affected by NQEs. This does not imply that all D₂O motions are classical, but rather that the competing NQEs on different degrees of freedom (vide infra) almost completely compensate each other; the D₂O rotational dynamics can then be correctly described by classical mechanics. (In contrast with the present q-TIP4P/F potential, typical force-fields like SPC/E or TIP4P-2005 already include an effective description of NQEs for H₂O; thus they cannot be adapted to D₂O by

1
2
3 simply changing the hydrogen atoms' mass.)
4

5 Water reorientation has been argued^{12,13} to proceed not by the traditional Debye diffusion
6 mechanism but rather via sudden large angular jumps when an OH group trades H-bond
7 acceptors (fig 2a). As we will later pursue, these jump H-bond exchanges can be seen as a
8 chemical reaction, breaking and making H-bonds.
9

10 Our quantum TRPMD simulations confirm that the jumps are still observed when NQEs
11 are included (see SI), and that their mechanism is very similar to that found in classical
12 simulations. Figure 2b shows that the H₂O classical and quantum-mechanical jump angle
13 distributions are practically identical. Since the jump amplitude $\Delta\theta$ is the angle formed by
14 the three oxygen atoms depicted in fig 2a,^{12,13} their large effective mass leads to very limited
15 quantum fluctuations.
16

17 Within the extended jump model^{12,13} (EJM) description, the τ_n reorientation rate (inverse
18 time) is the sum of the independent jump and frame reorientation rates. The reorientation
19 times are thus determined by the jump time τ_0 , defined as the inverse of the jump rate
20 constant, the jump amplitude $\Delta\theta$ and the slower H-bond complex frame reorientation time
21 between successive H-bond jumps. The latter is close to diffusive and is approximated
22 by $1/[D_R^{\text{frame}} n(n+1)]$, where D_R^{frame} is the frame rotational diffusion constant. When the
23 $P(\Delta\theta)$ jump angle distribution is explicitly considered, the EJM reorientation times are^{13,19}
24
25

26
27
28
29
30
31
32
33
34
35
36
37
38
39
40
41
42
43
44
45
46
47
48
49
50

$$\begin{aligned} \frac{1}{\tau_n^{\text{EJM}}} &= \frac{1}{\tau_n^{\text{jump}}} + \frac{1}{\tau_n^{\text{frame}}} \\ &= \frac{1}{\tau_0} \left[1 - \frac{1}{2n+1} \int_0^\pi d\Delta\theta P(\Delta\theta) \frac{\sin [(2n+1)\Delta\theta/2]}{\sin(\Delta\theta/2)} \right] \\ &\quad + D_R^{\text{frame}} n(n+1) . \end{aligned} \quad (2)$$

51 We have computed the ingredients of the EJM as described in ref 13, using a Stable States
52 approach to calculate τ_0 and a strict geometric H-bond definition (see SI). As described in SI,
53 very similar results are obtained with the PAMM²⁰ probabilistic H-bond definition. In the
54 quantum case, the ring-polymer centroids were used to calculate the jump rate constant.^{21,22}
55
56
57
58
59
60

The frame rotational diffusion constant D_R^{frame} was determined from the first and second order reorientation times for an intact H-bonded pair of water molecules (see SI). The resulting EJM reorientation times [eq 2] in Table 1 are seen to be in good agreement with the simulated τ_n values. This shows that the EJM initially suggested from an analysis of classical molecular dynamics^{12,13} also provides a good description of water reorientation when NQEs are included. Accordingly, we can now use the EJM to determine the origin of the isotope and nuclear quantum effects on water reorientation dynamics.

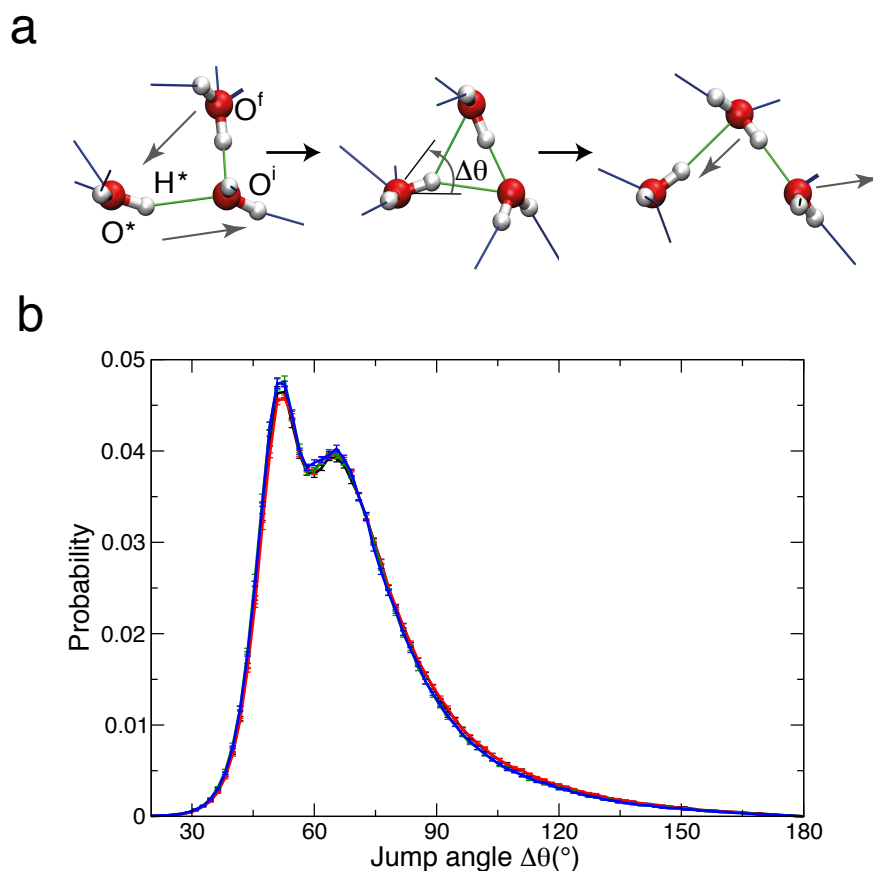


Figure 2: a) Water jump mechanism^{12,13} b) Distributions of jump angles $\Delta\theta$ calculated from classical H_2O (black), quantum H_2O (red), classical D_2O (green) and quantum D_2O (blue) simulations; all distributions strongly overlap.

Table 1 shows that the acceleration of H_2O reorientation dynamics induced by quantum effects is essentially caused by an acceleration in the jump dynamics (the frame reorientation

1
2
3 is accelerated to the same extent as the jumps, but remains much slower than the jumps in
4 the classical and quantum descriptions). The jumps are the dominant reorientation pathway
5 in both the classical and quantum cases, and the jump time τ_0 exhibits exactly the same
6 acceleration as do the τ_n reorientation times.
7
8
9
10

11 We can therefore now focus on the origin of the NQE on the jump time. We immediately
12 discard the possibility that a significant tunneling contribution could assist the water hydrogen
13 atom's jump between the initial and final H-bond acceptors. In agreement with the conclusion
14 of a preliminary study treating only the OH rotation quantum mechanically,¹³ our quantum
15 simulations show that the polymer beads' distribution at the jump transition state (see SI)
16 does not exhibit the bimodal behavior expected if tunneling were important.
17
18
19
20
21
22
23

24 In order to analyze and understand the NQE for the jump kinetics, we require a comparable
25 jump rate formulation for both the classical and quantum situations. In the classical case,
26 viewing, as in the previous section, the jump as a chemical reaction in which the H-bond
27 partners of the reorienting OH are exchanged, leads¹³ to the jump rate constant expression,
28 here written in terms of its inverse, the jump time τ_0^{cl}
29
30
31
32
33
34

$$\tau_0^{\text{cl}} = \frac{2\pi}{\omega^{\text{cl}}} \exp\left(\Delta G_{\text{cl}}^\ddagger/k_bT\right) . \quad (3)$$

35
36
37
38
39 Here ω^{cl} is the attempt frequency, i.e., the frequency of the reaction coordinate for the
40 reactant ($O^*H^* \cdots O^i$) configuration; $\Delta G_{\text{cl}}^\ddagger$ is the activation free energy for the exchange,
41 with the transition state (TS) defined by the O^*H^* in-plane libration at the midpoint of the
42 jump, with the two H-bonds of H^* to O^i and O^j of equal length (see fig 2a). $\Delta G_{\text{cl}}^\ddagger$ can be
43 decomposed into contributions from different coordinates in the passage from the reactant to
44 the TS.^{13,23} For the present q-TIP4P/F potential, the unstable reaction coordinate at the
45 TS is the $O^iO^*O^j$ anti-symmetric stretch compressing the new O^*O^j H-bond and expanding
46 the old O^*O^i H-bond. (With the SPC/E potential and other classical potentials, at the TS,
47 the in-plane O^*H^* libration has a double well potential and the reaction coordinate is this
48
49
50
51
52
53
54
55
56
57
58
59
60

libration.¹³) In the reactant, the reaction coordinate is the O^*O^f vibration (see SI). All other coordinates, including e.g. the O^*H^* libration, the O^*H^* stretch and the solvent motions are stable, transverse coordinates both in the reactant and at the TS.

Turning to the quantum description, the H-bond exchange rate constant is not conveniently couched in such explicit ingredients. However, as argued in the SI, the reaction coordinate in the reactant (the O^*O^f vibration) and at the TS (the $O^iO^*O^f$ anti-symmetric stretch) are well approximated as classical motions. In that case, we can employ an approach analogous to that used for proton transfer reactions,^{24,25} and write for the quantum case

$$\tau_0^{\text{qu}} = \frac{2\pi}{\omega^{\text{qu}}} \exp(\Delta G_{\text{qu}}^\ddagger/k_bT) \quad , \quad (4)$$

where the NQEs enter in the quantum free energy barrier $\Delta G_{\text{qu}}^\ddagger$, which includes the difference of the zero-point energies (ZPEs) of the transverse coordinates in the reactant and at the TS.

To expose the NQE's major ingredients, we will presently take the ratio of eqs 4 and 3. But first we decompose the activation free energy in more detail. $\Delta G_{\text{qu}}^\ddagger$ is the free energy change along the explicit H-bond-related reaction coordinate from reactant to TS, with all other, transverse, coordinates equilibrated to the reaction coordinate. (The actual dynamical path differs from this path, but this is irrelevant for the activation free energy calculation.) Since the classical and quantum mechanisms are the same, this is the free energy cost for the initial H-bond's elongation and for the final partner water molecule's approach to form the new H-bond.^{13,23} Finally, the SI shows that it is a good approximation to treat this barrier simply as the sum of the two independent contributions of the O^*O^i and O^*O^f modes,

$$\Delta G^\ddagger \simeq \Delta G_{\text{elong}}^\ddagger + \Delta G_{\text{compr}}^\ddagger \quad , \quad (5)$$

i.e., to treat these modes as decoupled; here $\Delta G_{\text{elong,compr}}^\ddagger$ are respectively the free energy costs for the elongation of the initial O^*O^i bond and for the compression of the O^*O^f distance.

Each term in the rhs of eq 5 corresponds to the free energy cost of bringing a pair of

1
2
3
4 water molecules from their initial, reactant state, separation to their TS separation. These
5
6 contributions can thus be straightforwardly determined from the potential of mean force
7
8 (pmf) along the O-O distance $W(r)$, which is related to the radial distribution function (rdf)
9
10 $g(r)$ between oxygen atoms, $W(r) = -k_B T \ln [g(r)]$. In the reactant state configuration, O^i
11
12 lies in the first hydration shell of O^* , so that the average $O^* - O^i$ separation is the distance
13
14 where the rdf exhibits its first peak $r_{\max 1}$ (fig 3). As for O^f , before the jump it lies on average
15
16 in the second shell¹³ of O^* , and the average $O^* - O^f$ separation is therefore the radius at
17
18 which the rdf exhibits its second peak, $r_{\max 2}$ (fig 3). At the jump TS, O^i and O^f are at the
19
20 same distance from O^* , which is that of the rdf's first minimum, r_{\min} (fig 3).

21
22 From this analysis, the free energy barrier eq 5 can thus be approximated as

$$23 \quad \Delta G^\ddagger \simeq [W(r_{\min}) - W(r_{\max 1})] + [W(r_{\min}) - W(r_{\max 2})] , \quad (6)$$

24
25 as illustrated in fig 3, and the classical and quantum jump times in eqs 3-4 can be estimated
26
27 from the classical and quantum O-O rdfs $g^{\text{cl,qu}}(r)$,

$$28 \quad \tau_0^{\text{cl,qu}} \simeq \frac{2\pi}{\omega^{\text{cl,qu}}} \frac{g^{\text{cl,qu}}(r_{\max 1})}{g^{\text{cl,qu}}(r_{\min})} \frac{g^{\text{cl,qu}}(r_{\max 2})}{g^{\text{cl,qu}}(r_{\min})} . \quad (7)$$

29
30 We have computed the O-O rdf from both the classical and quantum simulations. As was
31
32 originally found in pioneering quantum simulations of liquid water,^{5,6} Figure 4 shows that
33
34 while NQEs do not noticeably affect the D₂O rdf, they do lead to a decrease in the H₂O rdf
35
36 structure and thus to smaller pmf free energy barriers.

37
38 Recall from the discussion above eq 4 that the reaction coordinate comprises relative
39
40 classical motions of O^* and the oxygens of its initial and final H-bond partners; the quantum
41
42 pmf therefore differs from the classical pmf because it includes ZPE contributions from all
43
44 the *transverse* coordinates, which vary with the O-O distance. Accordingly, we now explain
45
46 the NQEs on the rdfs by considering the ZPEs of the three quantum H-bonding modes –
47
48 the OH stretch and the two librational modes – and how they change when the H-bond is
49
50
51
52
53
54
55
56
57
58
59
60

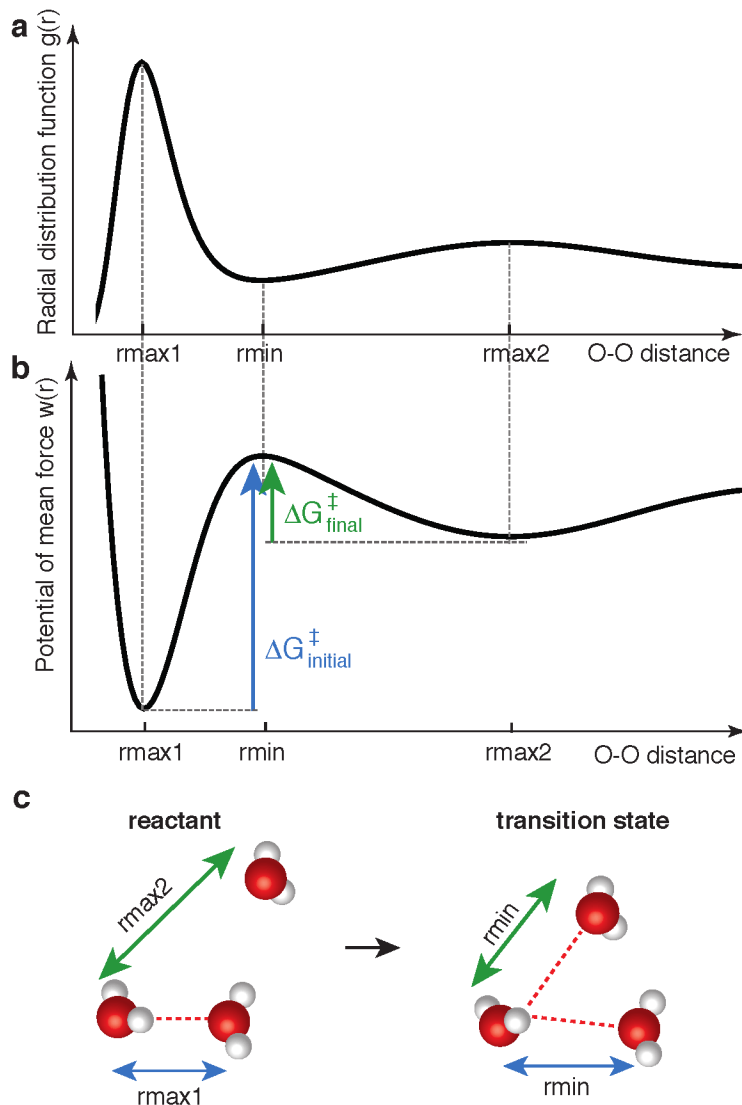


Figure 3: Schematic representation of the radial distribution function $g(r)$ (a) and potential of mean force (pmf) $W(r)$ (b) along the O-O distance between two water oxygen atoms, together with the key changes in the O-O distances during the jump (c). The $\Delta G_{\text{initial,final}}^{\ddagger}$ free energy barriers respectively associated with the elongation of the initial O^*O^i H-bond (blue) and the compression of the O^*O^f distance to the new H-bond partner initially lying in the second hydration shell (green) are shown on the pmf. See the text.

elongated. There are competing effects here: upon H-bond elongation, the H-bond acceptor attracts the H-bond donor quantum hydrogen atom H^* less strongly, so that with this now weaker H-bond, H^* becomes less delocalized along the stretch mode and the O^*H^* stretch ZPE increases. But this weaker H-bond situation also decreases the restoring torque on

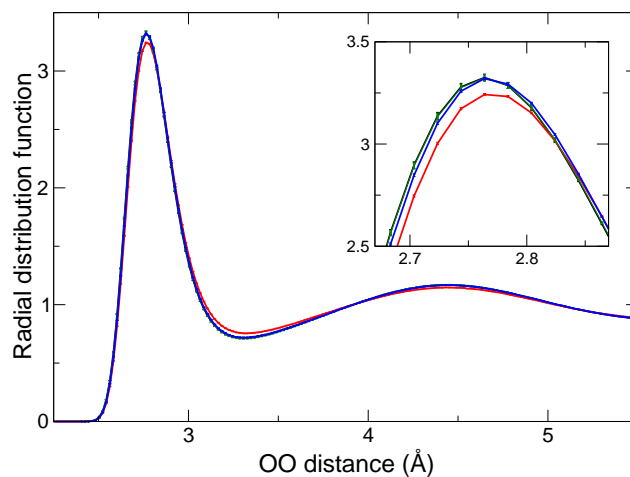


Figure 4: Radial distribution functions in classical H₂O (black), quantum H₂O (red), classical D₂O (green) and quantum D₂O (blue), where the inset focuses on the first peak region. The error bars give the Student 95% confidence interval determined from the results obtained on the set of independent trajectories. The classical H₂O and D₂O distributions are almost superimposed, while for the quantum distributions, there is a smaller barrier for H₂O than for D₂O.

the donor water molecule, which becomes more delocalized along the libration coordinate, whose ZPE thus decreases. Therefore, when the O-O distance increases, the stretch ZPE increases while the librational ZPE decreases. As was originally recognized in a non-reactive context^{7,8} and since been seen in several others,^{26–28} the NQEs on stretch and librational modes thus partly compensate each other. The overall decrease in the structure of the H₂O rdf induced by NQEs (fig 4) arises from the slightly dominant effect of the librational ZPE, which decreases the free energy barriers (see SI). These competing quantum effects are thus essential to obtain a good description of the overall NQE on the dynamics. A prior study²⁹ of quantum effects on water jump dynamics – which also indicated that the jump mechanism remained a correct water reorientation description – made two important approximations which compromise this picture of competing effects: spherical Gaussian wavepackets having the same width along the OH stretch and OH libration modes, and use of a water model with a harmonic OH stretch, in contrast with the present q-TIP4P/F model which accounts

for this mode's anharmonicity.

Nuclear quantum effects and isotope effects

We now analyze the change in the jump times between two systems, conveniently labeled a and b , which differ either by their description of nuclear dynamics – quantum vs. classical – or by their isotope – H₂O vs. D₂O. Equations 3,4 and (in particular) 7 show that the jump time can be described as the product of three terms, arising respectively from the frequency prefactor and from the change in the free energy costs to elongate the initial bond and compress the distance to the final acceptor, so that the ratio of a and b jump times has a corresponding product contribution with three ingredients:

$$\begin{aligned} \frac{\tau_0^a}{\tau_0^b} &= \rho_\omega \rho_{\text{elong}} \rho_{\text{compr}} \\ \rho_\omega &= \omega^b / \omega^a \\ \rho_{\text{elong}} &= e^{(\Delta G_{\text{elong}}^{\ddagger a} - \Delta G_{\text{elong}}^{\ddagger b}) / k_b T} = \frac{g^a(r_{\text{max}1}) g^b(r_{\text{min}})}{g^a(r_{\text{min}}) g^b(r_{\text{max}1})} \\ \rho_{\text{compr}} &= e^{(\Delta G_{\text{compr}}^{\ddagger a} - \Delta G_{\text{compr}}^{\ddagger b}) / k_b T} = \frac{g^a(r_{\text{max}2}) g^b(r_{\text{min}})}{g^a(r_{\text{min}}) g^b(r_{\text{max}2})}. \end{aligned} \quad (8)$$

Table 2 lists the contributions of each term in eq 8 and shows that it can quantitatively predict both the isotope and nuclear quantum effects on the jump dynamics from the subtle changes in the rdf (fig 4).

We first analyze the nuclear quantum effect, i.e., the ratio between the quantum and classical jump times. The ω attempt frequency depends on the reaction coordinate reduced mass and on the pmf curvature in the reactant region. Since NQEs do not change the reduced mass and induce very small changes in the pmf curvature (fig 4), $\rho_\omega \simeq 1$. The key result shown by Table 2 is that the NQE acceleration in H₂O jump dynamics is due to the remaining two factors in the product, i.e. comparable contributions from the easier elongation of the initial H-bond and from the more facile approach of the final H-bond partner. As described above, the lowering of these barriers for the O-O motions arises from the change in the OH

libration ZPE, which is partly compensated by the change in the OH stretch ZPE. Although the jump reaction coordinate involving the heavy O atoms is essentially classical, the free energy cost of its rearrangements is affected by these NQE contributions transverse to the reaction coordinate, since they change the interactions between the O atoms.

We now turn to the isotope effects, i.e. application of eq 8 for the ratio between the H₂O and D₂O jump times. The ρ_ω ratio is $\sqrt{18/20}$ since the reaction coordinate involves the motion of water molecules and not solely their hydrogen/deuterium atoms. However, Table 2 reveals that the simple picture³⁰ assigning the isotope effect for assorted measures of water dynamics to this trivial mass effect in the present case considerably underestimates the quantum acceleration from D₂O to H₂O. Most of this acceleration is found to arise from the change in the rdf, which leads to a decrease in the H-bond exchange free energy barriers. (Strictly speaking, one should consider the rdfs and pmfs along the distance between the water molecules' centers of mass, but as shown in the SI, these are almost indistinguishable from their analogues along the O-O distance.) This acceleration from D₂O to H₂O in the NQE is due to the different reduced ZPEs of the transverse coordinates in the heavier solvent.

Table 2: Isotope and nuclear quantum effects on the H-bond jump times τ_0 determined from our simulations and from eq 8, together with the three contributions in eq 8 (see SI).

		sim	eq 8	ρ_ω	ρ_{elong}	ρ_{compr}
τ_0^q/τ_0^c	H ₂ O	0.87	0.85	0.99	0.92	0.93
	D ₂ O	1.00	0.98	1.00	0.99	0.99
$\tau_0^{\text{H}_2\text{O}}/\tau_0^{\text{D}_2\text{O}}$	qm	0.79	0.82	0.95	0.93	0.93
	cl	0.90	0.94	0.95	0.99	0.99

Our results thus indicate that the mass of the isotope of the reorienting group is not the only factor that determines the isotope effect on the jump time, and that the further contributions from H-bond expansion and compression in eq 8 can be important. This feature is illustrated by ultrafast spectroscopy experiments where the OD group of an HOD molecule immersed in H₂O was measured to reorient faster than the OH group of an HOD in D₂O (2.5 ± 0.2 ps vs 3.0 ± 0.3 ps³¹). This result may seem surprising since the lighter OH

1
2
3
4 group might have been expected to reorient faster than the heavier OD. Although we did
5 not explicitly consider these isotopic mixtures here, our results show that the influence of
6 the isotopes present in the surrounding solvent makes a very important contribution to the
7 dynamics since they determine the free energy cost of the new partner's approach (and the
8 frame tumbling reorientation time^{12,13}).

9
10
11
12
13
14 Our study has shown that the jump picture for water reorientation applies in the nuclear
15 quantum mechanical description as well as in the classical regime. This has allowed us to
16 identify the molecular factors explaining the nuclear quantum and isotope effects on water
17 H-bond and reorientation dynamics. Nuclear quantum effects lead to a moderate water
18 dynamics acceleration, but do not affect the water reorientation mechanism, which mostly
19 proceeds through large angular jumps, just as in the classical case. The changes in the H-bond
20 jump dynamics are shown via a detailed jump perspective analysis to be semi-quantitatively
21 determined by the oxygen-oxygen radial distribution function changes. Our study thus
22 establishes a simple, robust, relationship between the liquid structure and the dynamics of
23 H-bond jumps, which are the elementary events governing water reorientation and – since
24 each H-bond jump induces translation of the water molecules involved – translation dynamics.
25
26
27
28
29
30
31
32
33
34
35
36
37

38 Acknowledgement

39
40
41 DMW thanks M. Rossi and M. Ceriotti for helpful discussions, and P. Gasparotto for advice
42 on the PAMM algorithm. Financial support from a CNRS – Royal Society international
43 collaborative grant (DEM, DL and JTH), the Agence Nationale de la Recherche (Grant
44 ANR-11-BSV5-027 to DL) and NSF (Grant CHE-1112564 to JTH) is acknowledged. DL
45 thanks for their hospitality DEM and his group at Oxford where this work was completed.
46
47
48
49
50
51
52
53

54 Supporting Information Available

55
56
57 The following files are available free of charge. Derivation of RPMD orientational time-
58
59
60

1
2
3 correlation functions. Further discussion of the librational contribution to the integrated
4 reorientation times, of the jump mechanism, of the PAMM H-bond analysis, of the correlated
5 $O^* - O^i$ and $O^* - O^f$ distribution functions, and of the OH stretch and librational ZPEs.
6
7
8
9

10 11 12 13 14 15 16 17 18 19 20 21 22 23 24 25 26 27 28 29 30 31 32 33 34 35 36 37 38 39 40 41 42 43 44 45 46 47 48 49 50 51 52 53 54 55 56 57 58 59 60

- (1) Ball, P. Water as an Active Constituent in Cell Biology. *Chem Rev* **2008**, *108*, 74–108.
- (2) Laage, D.; Stirnemann, G.; Sterpone, F.; Rey, R.; Hynes, J. T. Reorientation and Allied Dynamics in Water and Aqueous Solutions. *Annu Rev Phys Chem* **2011**, *62*, 395–416.
- (3) Levy, Y.; Onuchic, J. N. Water mediation in protein folding and molecular recognition. *Annu Rev Biophys Biomol Struct* **2006**, *35*, 389–415.
- (4) Berkelbach, T. C.; Tuckerman, M. E. Concerted Hydrogen-Bond Dynamics in the Transport Mechanism of the Hydrated Proton: A First-Principles Molecular Dynamics Study. *Phys Rev Lett* **2009**, *103*, 238302.
- (5) Kuharski, R. A.; Rossky, P. J. A quantum mechanical study of structure in liquid H₂O and D₂O. *J. Chem. Phys.* **1985**, *82*, 5164–5177.
- (6) Wallqvist, A.; Berne, B. J. Path-integral simulation of pure water. *Chem. Phys. Lett.* **1985**, *117*, 214–219.
- (7) Habershon, S.; Markland, T. E.; Manolopoulos, D. E. Competing quantum effects in the dynamics of a flexible water model. *J Chem Phys* **2009**, *131*, 024501.
- (8) Li, X.-Z.; Walker, B.; Michaelides, A. Quantum nature of the hydrogen bond. *Proc Natl Acad Sci* **2011**, *108*, 6369–6373.
- (9) Miller, T. F.; Manolopoulos, D. E. Quantum diffusion in liquid water from ring polymer molecular dynamics. *J. Chem. Phys.* **2005**, *123*, 154504.

- 1
2
3
4 (10) Paesani, F.; Iuchi, S.; Voth, G. A. Quantum effects in liquid water from an ab initio-based
5 polarizable force field. *J. Chem. Phys.* **2007**, *127*, 074506.
6
7
8
9 (11) Paesani, F.; Yoo, S.; Bakker, H. J.; Xantheas, S. S. Nuclear Quantum Effects in the
10 Reorientation of Water. *J. Phys. Chem. Lett.* **2010**, *1*, 2316.
11
12
13 (12) Laage, D.; Hynes, J. T. A Molecular Jump Mechanism of Water Reorientation. *Science*
14 **2006**, *311*, 832–835.
15
16
17
18 (13) Laage, D.; Hynes, J. T. On the Molecular Mechanism of Water Reorientation. *J. Phys.*
19 *Chem. B* **2008**, *112*, 14230–14242.
20
21
22
23 (14) Ludwig, R. The mechanism of the molecular reorientation in water. *Chemphyschem*
24 **2007**, *8*, 44–46.
25
26
27
28 (15) Rossi, M.; Ceriotti, M.; Manolopoulos, D. E. How to remove the spurious resonances
29 from ring polymer molecular dynamics. *J. Chem. Phys.* **2014**, *140*, 234116.
30
31
32
33 (16) Medders, G. R.; Babin, V.; Paesani, F. Development of a First-Principles Water Potential
34 with Flexible Monomers. III. Liquid Phase Properties. *J Chem Theory Comput* **2014**,
35 *10*, 2906–2910.
36
37
38
39
40 (17) Kell, G. S. Precise representation of volume properties of water at one atmosphere. *J*
41 *Chem Eng Data* **1967**, *12*, 66–69.
42
43
44
45 (18) Fogarty, A. C.; Duboué-Dijon, E.; Sterpone, F.; Hynes, J. T.; Laage, D. *Chem. Soc.*
46 *Rev.* **2013**, *42*, 5672–5683.
47
48
49
50 (19) Boisson, J.; Stirnemann, G.; Laage, D.; Hynes, J. T. Water reorientation dynamics in the
51 first hydration shells of F⁻ and I⁻. *Phys. Chem. Chem. Phys.* **2011**, *13*, 19895–19901.
52
53
54
55 (20) Gasparotto, P.; Ceriotti, M. Recognizing molecular patterns by machine learning: An
56 agnostic structural definition of the hydrogen bond. *J. Chem. Phys.* **2014**, *141*, 174110.
57
58
59
60

- 1
2
3
4
5
6
7
8
9
10
11
12
13
14
15
16
17
18
19
20
21
22
23
24
25
26
27
28
29
30
31
32
33
34
35
36
37
38
39
40
41
42
43
44
45
46
47
48
49
50
51
52
53
54
55
56
57
58
59
60
- (21) Craig, I. R.; Manolopoulos, D. E. Chemical reaction rates from ring polymer molecular dynamics. *J Chem Phys* **2005**, *122*, 084106.
- (22) Craig, I. R.; Manolopoulos, D. E. A refined ring polymer molecular dynamics theory of chemical reaction rates. *J Chem Phys* **2005**, *123*, 34102.
- (23) Stirnemann, G.; Laage, D. Direct Evidence of Angular Jumps During Water Reorientation Through Two-Dimensional Infrared Anisotropy. *J Phys Chem Lett* **2010**, *1*, 1511–1516.
- (24) Kiefer, P. M.; Hynes, J. T. Nonlinear Free Energy Relations for Adiabatic Proton Transfer Reactions in a Polar Environment. I. Fixed Proton Donor/Acceptor Separation. *J Phys Chem A* **2002**, *106*, 1834–1849.
- (25) Kiefer, P. M.; Hynes, J. T. Nonlinear Free Energy Relations for Adiabatic Proton Transfer Reactions in a Polar Environment. II. Inclusion of the Hydrogen Bond Vibration. *J Phys Chem A* **2002**, *106*, 1850–1861.
- (26) Markland, T. E.; Berne, B. J. Unraveling quantum mechanical effects in water using isotopic fractionation. *Proc Natl Acad Sci U S A* **2012**, *109*, 7988–7991.
- (27) Liu, J.; Andino, R. S.; Miller, C. M.; Chen, X.; Wilkins, D. M.; Ceriotti, M.; Manolopoulos, D. E. A Surface-Specific Isotope Effect in Mixtures of Light and Heavy Water. *J Phys Chem C* **2013**, *117*, 2944–2951.
- (28) Wilkins, D. M.; Manolopoulos, D. E.; Dang, L. X. Nuclear quantum effects in water exchange around lithium and fluoride ions. *J. Chem. Phys.* **2015**, *142*, 064509.
- (29) Ono, J.; Hyeon-Deuk, K.; Ando, K. Semiquantal molecular dynamics simulations of hydrogen-bond dynamics in liquid water using spherical gaussian wave packets. *Int J Quant Chem* **2013**, *113*, 356–365.

- 1
2
3
4 (30) Ceriotti, M.; Fang, W.; Kusalik, P. G.; McKenzie, R. H.; Michaelides, A.; Morales, M. A.;
5 Markland, T. E. Nuclear Quantum Effects in Water and Aqueous Systems: Experiment,
6 Theory, and Current Challenges. *Chem Rev* **2016**, *116*, 7529–7550.
7
8
9
10 (31) Bakker, H. J.; Rezus, Y. L. A.; Timmer, R. L. A. Molecular reorientation of liquid
11 water studied with femtosecond midinfrared spectroscopy. *J Phys Chem A* **2008**, *112*,
12 11523–11534.
13
14
15
16
17
18
19
20
21
22
23
24
25
26
27
28
29
30
31
32
33
34
35
36
37
38
39
40
41
42
43
44
45
46
47
48
49
50
51
52
53
54
55
56
57
58
59
60